nature plants

SUPPLEMENTARY INFORMATION

DOI: 10.1038/NPLANTS.2015.87

Clustering of a kinesin-14 motor enables processive retrograde microtubule-based transport in plants

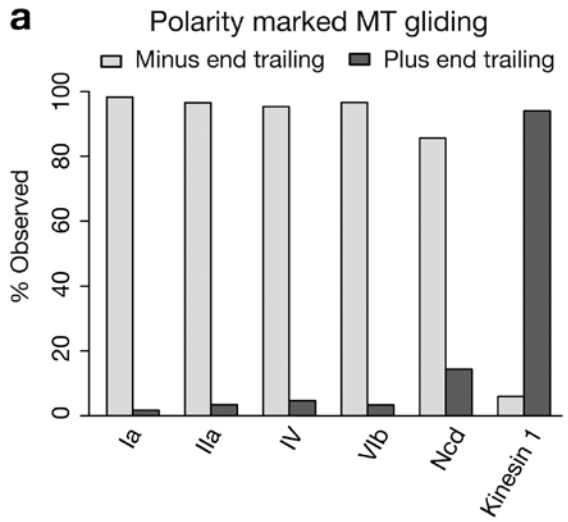

b

Gel filtration data

Motor	MW (kDa)	V_e - V_o (mL)
Ia	79.9	3.13
IIa	79.9	3.23
IIIa	91.1	NA
IV	81.0	5.48
Va	92.7	NA
VIb	79.9	2.99
VIb FL	188	1.8
NCD	81.0	3.04

V_e = elution volume
V_o = void volume

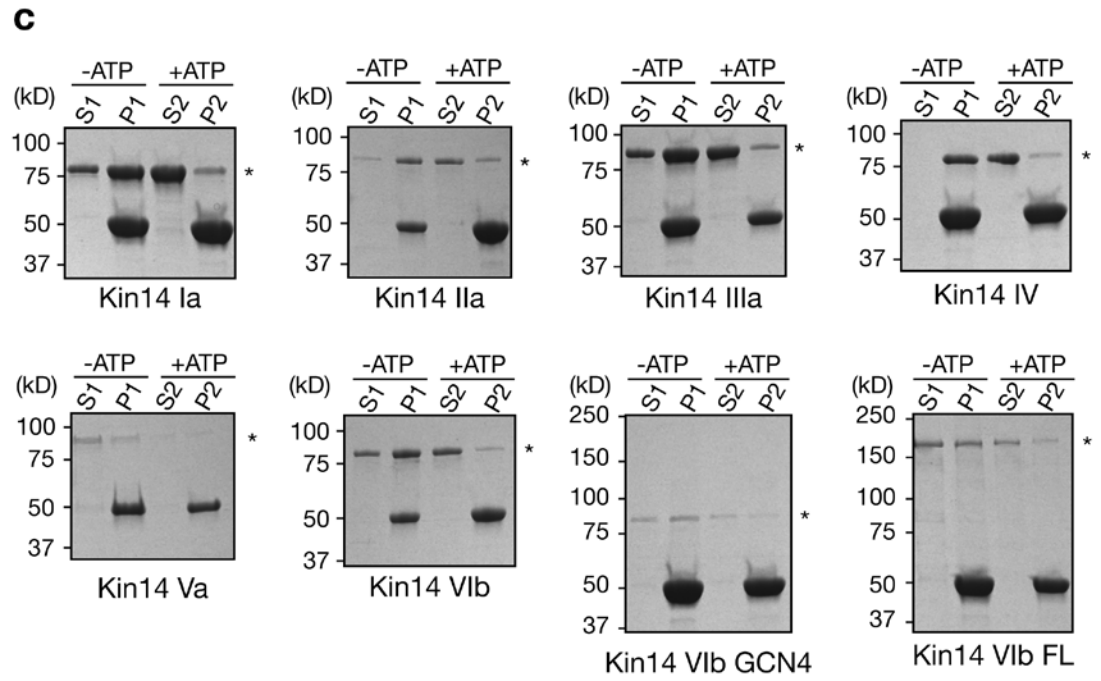

Figure S1. Additional *P. patens* kinesin-14 characterization
(a) The MT gliding assay using the polarity-marked MT showed that *P. patens* kinesin-14s have a retrograde polarity. Directionality of >100 polarity-marked MTs were scored and plotted in the figure for each motor. *Drosophila* Ncd and human kinesin-1 (K560) motors served as the control minus-end-directed and plus-end-directed motors, respectively. (b) Motor proteins were run on an S200 gel filtration column and retention volumes were measured and plotted. Tabulated values are elution volume minus void volume (~8 ml for this column). (c) Representative MT bind-and-release data (see Methods) for the motors used in this study. Motors were bound to MTs in the absence of ATP and dissociated from MTs by addition of ATP. Asterisks indicate location of motor band. A peculiar case was kin14-Va, which appeared to have little interaction with MTs, which is consistent with results on the *Arabidopsis* orthologue [S1].

DOI: 10.1038/NPLANTS.2015.87

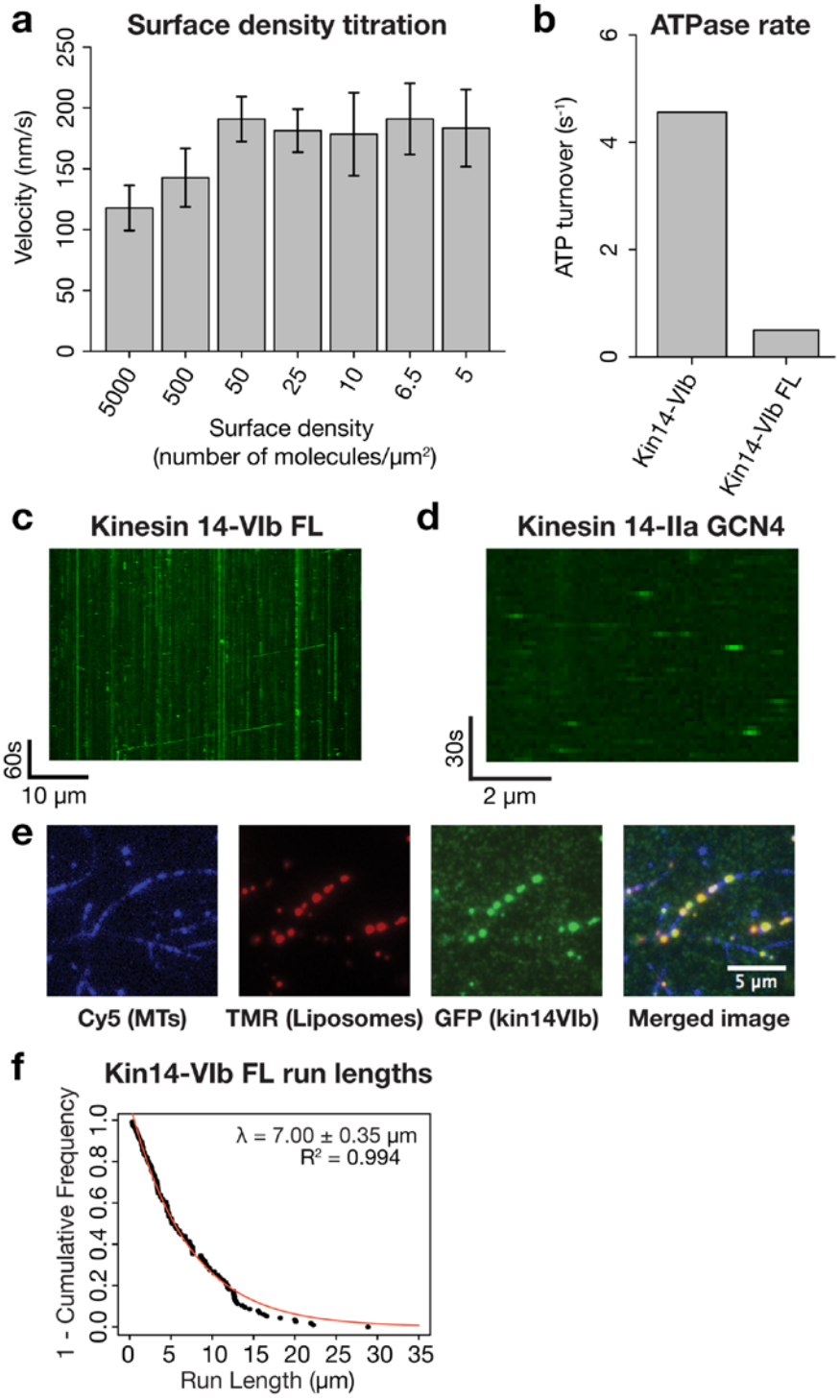

Figure S2. Kin14-VIb full-length is non-processive on its own, but transports liposomes for long distance
(a) Gliding velocity as a function of motor surface density for kin14-VIb. For densities lower than 5 motors/μm2 the MTs did not glide readily and appeared diffusive. Error bars represent SDs of at least 100 motile MTs. (b) Values for the MT stimulated rate of ATP hydrolysis for both the truncated and full-length form of Kin14-VIb at a saturating MT density (20 μM). (c) A kymograph for a single molecule fluorescence assay for GFP-kin14-VIb FL (~1 nM). The majority of the GFP signals were not motile. However, a few processive runs were also visible (visible as diagonal lines). These particles were brighter than most of their surrounding GFP particles, indicating that they are likely small aggregates. (d) A kymograph for a single molecule fluorescence assay for GFP-kin14-IIa motor tetramerized by the GCN4 motif. Tetramerized kin14-IIa did not exhibit processive motility. (e) Bright GFP-kin14-VIb signal observed on moving liposomes due to high motor density. (f) Transport length data for liposomes coated with full-length kin14-VIb. The data points were fit to an exponential with a fit parameter of $\lambda = 7.00 \pm 0.35$ μm (error is determined from goodness of fit parameters; R2 = 0.994; n = 116 moving particles).

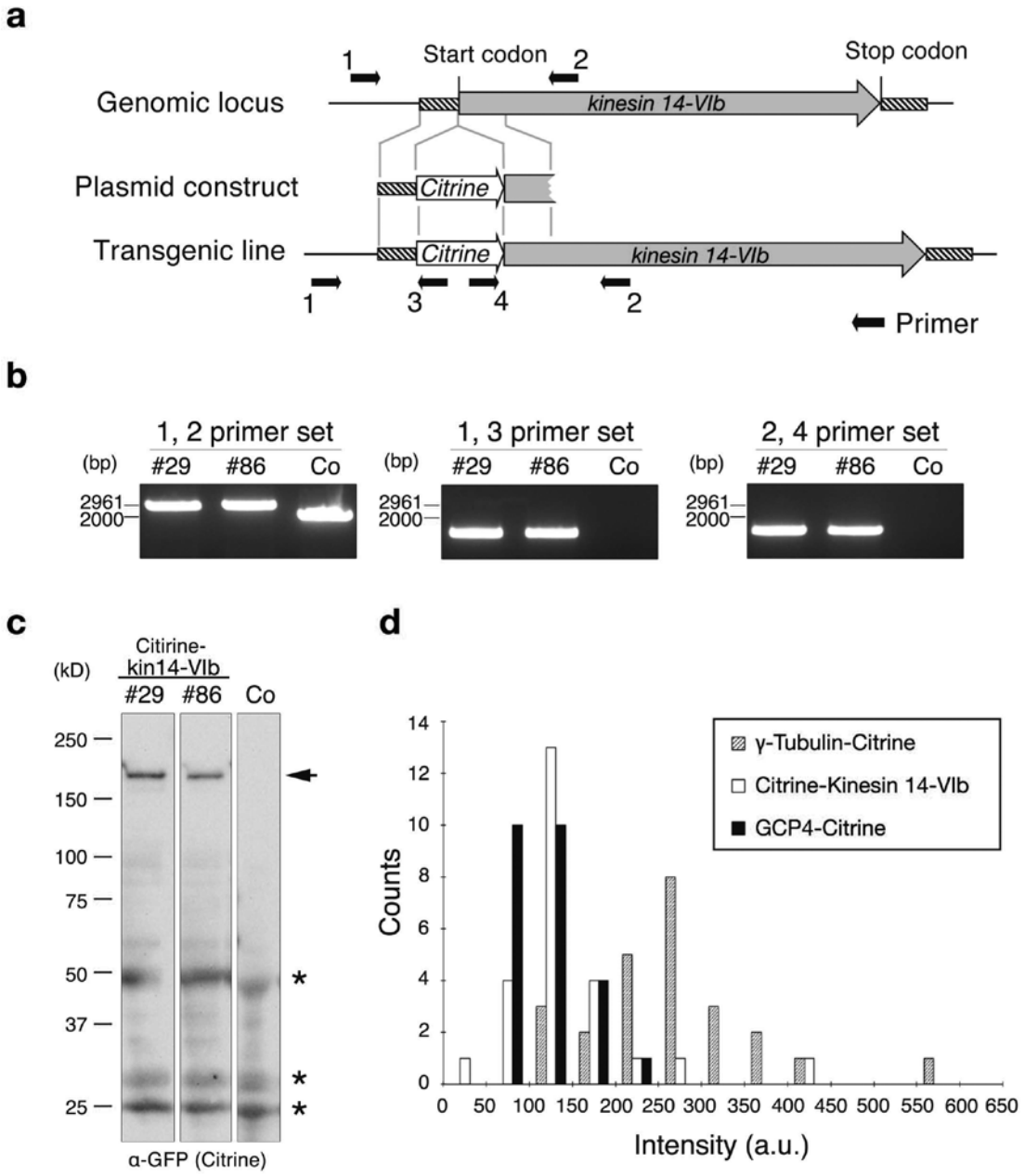

Figure S3. Establishment of the kin14-VIb replacement line
(a) Scheme of the transgenic line selection (see [S2] for details). The N-terminus of the endogenous *kin14-VIb* gene was tagged with the *Citrine* gene via homologous recombination. Note that no other sequences, including the selection marker gene, were integrated in this line. Arrows indicate the locations of the PCR primers used in (b). (b) Homologous recombination was confirmed by 3 sets of PCR. "Co" stands for a control line, in which the *Citrine* gene is not integrated. (c) Expression of Citrine-kin14-VIb was confirmed by immunoblotting with the anti-GFP antibody, which also recognized Citrine. Arrow indicates the band corresponding to Citrine-kin14-VIb, whereas non-specific bands are marked with asterisks. "Co" stands for a control line, in which the *Citrine* gene is not integrated. (d) Comparison of the signal intensities of Citrine-kin14-VIb, γ-tubulin-Citrine-b and GCP4-Citine. In *P. patens*, a single GCP4 gene is present, whereas two γ-tubulin genes are expressed in protonemata (γ-tubulin-a and -b). The γ-tubulin-Citrine intensity was measured using the γ-tubulin-b-Citrine /γ-tubulin-aΔ /mCherry-tubulin line, in which all the γ-tubulin in the cells were expected to have the Citrine tag [S3]. Because of the autofluorescence derived from the chloroplast, the background signal: were not uniform within the cell. Therefore, we selected the same region as where the Citrine signals appeared, and measured the background signal intensity 3 frames before the Citrine signal appeared or 3 frames after the Citrine signals disappeared.

DOI: 10.1038/NPLANTS.2015.87

Table S1. List of PCR primers used in this study

Plasmid	Gene	5' primer	3' primer
pGG839 (pET15b)	Kin14-Ia (349–795 a.a.)	TTTGCGGCCGCCGGCAAGT CTGTGGCCGAGATC	AAACTCGAGCTAACTTGAACG AATGCTCAAGG
pGG846 (pET15b)	Kin14-IIa (500–1033 a.a.)	TTTGCGGCCGCCGTGCAAG TGCTGAGGAATGAAC	AAAGGATCCTTACCTGGACTT ATACTTCTCC
pGG845 (pET15b)	Kin14-IIIa (529–1070 a.a.)	TTTGCGGCCGCCCTGCGTG AAGATTTGTGCGCGA	AAAGGATCCTTACTCGACTAC CAACTTTTCC
pGG844 (pET15b)	Kin14-IV (90–537 a.a.)	TTTGCGGCCGCCTCATTGTC TTCAAGCTCCGATG	AAAGGATCCTTATGGATTGGT AGTGAATGAAG
pGG851 (pET15b)	Kin14-Va (1–556 a.a.)	TTTGCGGCCGCCATGGGGG ATGCAGCAGAATTGCGGT	AAAGGATCCTTATTCGTGGCT AGTAAGATCAGC
pGG840 (pET15b)	Kin14-VIb (851–1322 a.a.)	TTTGCGGCCGCCAGAGATG ATTTGAGGGGACG	AAAAGATCTTTAATCTGCAGT TTTGATTCC
pGG957 (pFastBacHT)	Kin14-IIa full-length	TTACTAGTGATGGATGTGG CAAGAATGG	TTGGTACCTTACCTCCAAGAG GTTGAGG
pGG960 (pFastBacHT)	Kin14-VIb full-length	TTACTAGTGATGGCCTCGG ATGCATCTCACG	TTGGTACCTTAATCTGCAGTTT TGATTCC
pMN590 (Citrine tagging vector)	Kin14-VIb	AAAGGTACCCAAGTGTATG TCACTCTGCAATCC	AAACTCGAGTTTATTCTCCGCC ACGACCACCC
		AAAACTAGTTATGGCCTCG GATGCATCTCACGTC	AAAAGCGGCCGCCCACAAGAA AAGTGTATGTCGCTGGCTG

Restriction enzyme sites are marked with underlines. *EGFP* was inserted at the NdeI site of the 6×His-containing vector pET15b (the NotI site was added at the C-terminus of the *EGFP* gene). The following linker sequences were inserted between GFP and kin14: HRYTSLYKKAGSAAA (motor constructs), QDPEFKGLRRSTSSLV (full-length constructs), or HRYTSLYKKAGSAIEDKLEEILSKLYHIENELARIKKLLGEIGGGSGGGSAAA (GCN4 tetramer construct).

References

[S1] Suetsugu, N. *et al.* Two kinesin-like proteins mediate actin-based chloroplast movement in Arabidopsis thaliana. *Proc Natl Acad Sci U S A* 107, 8860-8865, doi:10.1073/pnas.0912773107 (2010).

[S2] Yamada, M., Miki, T. & Goshima, G. Imaging mitosis in the moss Physcomitrella patens. *Methods Mol Biol*. In press (2015).

[S3] Nakaoka, Y., Kimura, A., Tani, T. & Goshima, G. Cytoplasmic Nucleation and Atypical Branching Nucleation Generate Endoplasmic Microtubules in Physcomitrella patens. *Plant Cell* 27, 228-242, doi:10.1105/tpc.114.134817 (2015).

DOI: 10.1038/NPLANTS.2015.87

Supplementary movie legends

Movie 1. Polarity and gliding properties of GFP-kin14 constructs

Polarity marked MT gliding assay (minus end in red) for active kinesin-14s.

Movie 2. Kin14-VIb GCN4 tetramer moves processively along MTs

GFP-kin14-VIb GCN4 tetramers (green spots) are seen moving along MTs (blue).

Movie 3. Kin14-VIb-coated liposome transport assay

Kin14-VIb-coated liposomes (red) translocating along MTs (blue). Some liposomes switch between MT tracks, which is likely due to multiple motors on their surface.

Movie 4. *In vivo* motility of clustered Citrine-kin14-VIb

The Citrine (green) and mCherry-tubulin (magenta) images were acquired every 0.2 s in the endoplasm of a protonemal cell. Note that autofluorescence derived from chloroplasts are also visible (green). Inset highlights a moving Citrine-kin14-VIb signal along the MT (Citrine images were acquired every 0.12 s, whereas mCherry-tubulin was imaged at one time-point).